Biochimica et Biophysica Acta 1798 (2010) 471–481

Contents lists available at ScienceDirect

Biochimica et Biophysica Acta

journal homepage: www.elsevier.com/locate/bbamem

Sphingomyelin-rich domains are sites of lysenin oligomerization: Implications for raft studies

Magdalena Kulma [a], Monika Hereć [a], Wojciech Grudziński [b], Gregor Anderluh [c], Wiesław I. Gruszecki [b], Katarzyna Kwiatkowska [a], Andrzej Sobota [a,*]

[a] Department of Cell Biology, The Nencki Institute of Experimental Biology, 3 Pasteur St., 02-093 Warsaw, Poland
[b] Department of Biophysics, Institute of Physics, Maria Curie-Sklodowska University, 20-031 Lublin, Poland
[c] Department of Biology, Biotechnical Faculty, University of Ljubljana, 1000 Ljubljana, Slovenia

ARTICLE INFO

Article history:
Received 12 August 2009
Received in revised form 28 November 2009
Accepted 8 December 2009
Available online 16 December 2009

Keywords:
Raft
Pore-forming toxin
Sphingomyelin
Plasma membrane
Protein oligomerization

ABSTRACT

Lysenin is a self-assembling, pore-forming toxin which specifically recognizes sphingomyelin. Mutation of tryptophan 20 abolishes lysenin oligomerization and cytolytic activity. We studied the interaction of lysenin WT and W20A with sphingomyelin in membranes of various lipid compositions which, according to atomic force microscopy studies, generated either homo- or heterogeneous sphingomyelin distribution. Liposomes composed of SM/DOPC, SM/DOPC/cholesterol and SM/DPPC/cholesterol could bind the highest amounts of GST-lysenin WT, as shown by surface plasmon resonance analysis. These lipid compositions enhanced the release of carboxyfluorescein from liposomes induced by lysenin WT, pointing to the importance of heterogeneous sphingomyelin distribution for lysenin WT binding and oligomerization. Lysenin W20A bound more weakly to sphingomyelin-containing liposomes than did lysenin WT. The same amounts of lysenin W20A bound to sphingomyelin mixed with either DOPC or DPPC, indicating that the binding was not affected by sphingomyelin distribution in the membranes. The mutant lysenin had a limited ability to penetrate hydrophobic region of the membrane as indicated by measurements of surface pressure changes. When applied to detect sphingomyelin on the cell surface, lysenin W20A formed large conglomerates on the membrane, different from small and regular clusters of lysenin WT. Only lysenin WT recognized sphingomyelin pool affected by formation of raft-based signaling platforms. During fractionation of Triton X-100 cell lysates, SDS-resistant oligomers of lysenin WT associated with membrane fragments insoluble in Triton X-100 while monomers of lysenin W20A partitioned to Triton X-100-soluble membrane fractions. Altogether, the data suggest that oligomerization of lysenin WT is a prerequisite for its docking in raft-related domains.

1. Introduction

Sphingomyelin is a major lipid of the plasma membrane located mainly in its outer leaflet. Due to the high content of saturated acyl chains, sphingomyelin together with glycolipids and cholesterol forms microdomains, named rafts [1,2]. The content of sphingomyelin in rafts exceeds by 20–30% that in the bulk of the plasma membrane as found by mass spectrometry analysis [3,4]. The unique lipid environment of rafts facilitates local accumulation of distinct proteins, including those anchored in the outer leaflet by a glycosylphosphatidylinositol moiety, and Src family kinases docked in the inner leaflet of rafts via saturated fatty acid residues [5–7]. The dense packing of lipid molecules within raft renders them resistant to solubilization in non-ionic detergents, a property used widely for biochemical studies of raft composition and function [8,9]. Ample data indicate that rafts serve as signaling platforms for various receptors, among which immunoreceptors and death receptors are the most thoroughly studied in terms of their association with rafts for signal generation [10–12]. It has been found that activation of TNF receptor family members and immunoreceptor FcγRIIA triggers so-called sphingomyelin cycle which starts from sphingomyelin hydrolysis yielding ceramide. The ceramide favors clustering of the receptors in the plane of the plasma membrane and their association with rafts, but the lipid also serves as an intracellular second messenger [12–16].

The structural and signaling roles of sphingomyelin imply the existence of various pools of the lipid in the plasma membrane, as indicated also by scarce experimental data [17,18]. Studies on raft and non-raft sphingomyelin and its dynamics are likely to be facilitated by application of sphingomyelin-specific probes, such as equinatoxin II, lysenin and lysenin-related proteins [19–21]. Lysenin is a 297 amino acid-long toxin originating from the coelomic fluid of the earthworm *Eisenia foetida* which specifically recognizes sphingomyelin among lipids [22–24]. These data are in line with other biophysical studies on the interaction of lysenin with sphingomyelin showing that the

* Corresponding author. Tel.: +48 22 5892 234; fax: +48 22 822 5342.
E-mail address: a.sobota@nencki.gov.pl (A. Sobota).

0005-2736/$ – see front matter © 2009 Elsevier B.V. All rights reserved.
doi:10.1016/j.bbamem.2009.12.004

protein preferentially binds assemblies of sphingomyelin in the membrane [25]. Yet, the application of lysenin for studies of sphingomyelin organization in the plasma membrane is hindered by the lytic activity of the protein. Upon sphingomyelin binding, lysenin forms stable hexamers detectable by SDS-gel electrophoresis and electron microscopy. Oligomerization of lysenin is facilitated by cholesterol which increases fluidity of sphingomyelin-containing membranes and promotes separation of sphingomyelin-rich liquid-ordered phase [26–28]. Lysenin hexamers, formed in the sphingomyelin-containing membranes, are responsible for the channel activity of the toxin and its lytic property [28]. The recognition of sphingomyelin by lysenin and effective membrane-binding is of complex nature and requires participation of five of the six tryptophan residues scattered throughout the polypeptide [23,29]. Mutation of tryptophan 20 resulted in a loss of oligomerization and of the cytolytic activity of lysenin with maintenance of sphingomyelin binding [28]. Due to the lack of the lytic activity, the mutant lysenin W20A is of interest as a potential probe for studying sphingomyelin organization in the plasma membrane of living cells.

Recently, a truncated form of lysenin devoid of 160 N-terminal amino acids, named non-toxic protein, was used to analyze distribution of sphingomyelin in the plasma membrane of Jurkat cells. The sphingomyelin pool recognized by this truncated lysenin was spatially and functionally separated from GM1- and T cell receptor-enriched rafts [30]. It is not known, however, whether monomers of the non-toxic lysenin have the same sphingomyelin binding properties as the wild-type lysenin. Here we used GST-lysenin WT and GST-lysenin W20A to examine if both forms of the protein recognize assemblies of sphingomyelin in membranes. Determining whether homo- or heterogeneous distribution of sphingomyelin in the membrane favors/disfavors sphingomyelin recognition by WT and W20A lysenin should indicate whether the two proteins target the same pool of sphingomyelin in the plasma membrane. Our data indicate that W20A mutation has deprived lysenin of its ability to bind preferentially sphingomyelin clusters in membranes. Accordingly, fractionation of Triton X-100 lysates of cells revealed that GST-lysenin WT, but not GST-lysenin W20A, bound exclusively to sphingomyelin located in plasma membrane fragments resistant to the detergent, which pointed to their raft origin.

2. Materials and methods

2.1. Plasmids and protein purification

The plasmids expressing lysenin WT and lysenin W20A with a glutathione-S-transferase (GST) tag at the N-terminus were generated from pT7RS-lysenin WT and pT7RS-lysenin W20A templates, which were constructed as described before [28]. The cDNA fragments encoding the two proteins were amplified by PCR and subcloned to the pGEX-4T-3 vector (Amersham) using *Eco*RI/*Bam*HI restriction sites. For preparation of GST protein, empty pGEX-4T-3 vector was used. *Escherichia coli* was transformed with corresponding plasmids and the recombinant proteins were purified on a glutathione-agarose column according to manufacturer's instructions (Sigma).

2.2. Surface plasmon resonance (SPR)

The analysis was conducted at 25 °C on a BIAcore X apparatus (BIAcore, GE Healthcare) equipped with an L1 chip coated with large unilamellar vesicles (LUV) of various lipid compositions. Bovine brain semi-synthetic sphingomyelin (SM), cholesterol, dioleoyl phosphatidylcholine (DOPC), dipalmitoyl phosphatidylcholine (DPPC) were from Avanti Polar Lipids and Sigma. Appropriate mixtures of lipids: SM/DOPC or SM/DPPC at molar ratio 1:1 with or without cholesterol equimolar to SM, DOPC/cholesterol or DPPC/cholesterol at molar ratio 1:1, and DOPC or DPPC alone, were dried from chloroform:methanol (1:1, v:v) on a rotavapor for 3 h. The lipid film was resuspended in buffer A (150 mM NaCl, 30 mM Tris, pH 8.0), vortexed and freeze–thawed six times. The resulting multilamellar vesicles were extruded through polycarbonate filters with 100 nm pores to create LUV. The concentration of lipids with a choline head group was determined with Phospholipids B Kit (Wako Chemicals, Germany) and kept at 2 mM. The chip was first equilibrated with filtered and degassed running buffer A. Prior to coating with LUV, the surface of the chip was cleaned with three consecutive injections of isopropanol/50 mM NaOH (2:3, v:v) for 1 min at 30 μl/min. Liposomes were deposited on the chip at a low flow rate of 1 μl/min for 10 min. The amount of deposited liposomes corresponded to 700–900 resonance units (RU). Binding experiments were performed with 2 μM solution of GST-lysenin WT, GST-lysenin W20A or GST in buffer A applied at a flow rate of 30 μl/min. After 300 s (association phase) deposited material was washed with buffer A for another 300 s (dissociation phase).

2.3. Surface pressure measurements

The experiments were carried out with a NIMA Technology tensiometer model PS3 (Coventry, UK) at 23 ± 1 °C in darkness under argon atmosphere, essentially as described earlier [31]. The lipid composition of monolayers was: SM/DOPC/cholesterol at molar ratio 3:7:3 or DOPC/cholesterol at molar ratio 7:3. The total phospholipid concentration was 1 mM. The measurements of surface pressure as a function of time allows the membrane insertion kinetics to be determined by applying the following exponential equation:

$$(\pi - \pi_0)/(\pi_\infty - \pi_0) = A\left(1 - e^{-\alpha t}\right) + (1 - A)\left(1 - e^{-\beta t}\right) \quad (1)$$

where π, π_o, π_∞ are values of the surface pressure at time t (π), at the moment of injection of the protein (1–30 nM) to the aqueous subphase (π_o), and the plateau (π_∞), A is a pre-exponential factor, and α and β are the rate constants of the fast and slow phase of protein adsorption at the interface. The average rate constant Q represents relative efficiency of insertion calculated as

$$Q = A \cdot \alpha + (1 - A) \cdot \beta. \quad (2)$$

2.4. Atomic force microscopy measurements

Imaging was performed at 23 °C using a Nanosurf easyScan 2 AFM system. First, a monolayer composed of pure stearic acid prepared by repeated crystallization was deposited onto the mica surface by the Langmuir–Blodgett technique with a speed of lift of 1 mm/min. Monolayers composed of SM/DOPC/cholesterol or SM/DPPC/cholesterol (molar ratio 3:7:3), SM/DOPC or SM/DPPC (molar ratio 3:7) with 1 mM total phospholipid concentration were pre-formed on the surface of a buffer (150 mM NaCl, 50 mM Tris, pH 8.0) in a Teflon trough at the surface pressure of 21 mN/m and maintained constant by computer control. Monolayers were next deposited on the mica-stearic acid support and dried. This experimental design created mica surface exposing the hydrophobic fatty acyl chains of stearic acid for interaction with fatty acyl chains of lipids from the examined monolayers. Consequently, the monolayers oriented themselves with the lipid polar headgroups toward the environment. Images were taken in the dynamic mode with a silicon cantilever with a spring constant of 48 N/m and a tip with a radius of curvature less than 10 nm. The scanning rate was 1 Hz and 256 × 256 data points were acquired. Image data were flattened after acquisition.

2.5. Carboxyfluorescein release from LUV

LUV composed of SM/DOPC or SM/DPPC (molar ratio 3:7) with or without cholesterol equimolar to SM were prepared as described

above with the exception that lipid films were resuspended in buffer A at pH 7.6, containing 50 mM 6-carboxyfluorescein (Sigma). LUV were separated from external dye by pelleting (10 min, 10,000*g*, 25 °C) and suspended in buffer A (pH 7.6). The total concentration of phospholipids in the suspension was 1 mM; 0.5 ml of the LUV suspension was placed in a cuvette. Measurements were done on a Spex spectrofluorimeter (Jobin-Yvone) at Em/Ex = 490/520 nm (25 °C). Before adding proteins, fluorescence was monitored for 10 min to establish level of spontaneous efflux of the dye (F_i). Subsequently, at time set as 0, GST-lysenin WT or GST-lysenin W20A was added to LUV suspension (100 nM final protein concentration) and the fluorescence (F) was measured during 10 min (25 °C). The maximal efflux of 6-carboxyfluorescein (F_f) was determined in the presence of 0.1% Triton X-100. The results were expressed as % dye leakage = $100(F-F_i)/(F_f-F_i)$, according to ref [32].

2.6. Localization of lysenin, FcγRIIA and tyrosine-phosphorylated proteins at the plasma membrane

Transfected BHK cells stably expressing FcγRIIA were incubated with mouse anti-FcγRIIA IgG2b (clone IV.3, ATCC) for 20 min at 4 °C and either fixed with 3% paraformaldehyde to maintain non-activated receptor or incubated with goat anti-mouse IgG-Texas Red (Jackson ImmunoResearch) (15 min, 4 °C) to cross-link and activate the receptor [10]. After fixation cells were treated with 50 mM NH_4Cl, blocked with 3% fish gelatine and incubated with 20 nM GST-lysenin WT or 200 nM GST-lysenin W20A (30 min, 25 °C). After washing, the cells were exposed to rabbit anti-lysenin IgG (30 min, 25 °C) followed by goat anti-rabbit IgG-FITC (Rockland). Non-activated cells were additionally incubated with goat anti-mouse IgG-Texas Red to visualize FcγRIIA. To visualize tyrosine-phosphorylated proteins, fixed cells were permeabilized either with 0.05% Triton X-100 (5 min, 4 °C) or 0.005% digitonin (10 min, 25 °C), incubated with 3% fish gelatine (twice for 30 min, 25 °C) and treated with rabbit anti-phosphotyrosine IgG (Transduction Laboratories) and goat anti-rabbit IgG-FITC (1 h each incubation, 25 °C). In a series of experiments, cells were exposed to Triton X-100 or digitonin prior to labeling of lysenin on the cell surface as above. The samples were mounted in Mowiol/DABCO (1,4-diazabicyclo[2,2,2]-octane) and examined under a Nikon fluorescence microscope equipped with a DXM 120 °C digital camera and analyzed for protein clustering using ImageJ software (NIH) as described [33]. For each variant of experiment 10–12 cell images were analyzed from two independent experiments.

For colocalization analysis, confocal imaging was performed on a Leica microscope (TCS SP5) equipped with a 100X, N.A. 1.4 objective. FITC and Texas Red conjugated with appropriate antibodies were excited with 488 nm Ar and 594 nm HeNe lasers, respectively, in the mode of sequential excitation to exclude cross-over of their fluorescence. Stacks of 5–7 confocal planes (at 0.2 μm step) with a 4.5 zoom factor were acquired for each analyzed cell with attention paid to regions encompassing flat lamellae. The settings of photomultipliers were adjusted to obtain comparable ranges of pixel intensity in each channel (mean intensity values about 20 on a scale from 0 to 255), the speed of scanning was 200 Hz, scan resolution 1024x1024 pixels. Colocalization analysis was performed according to [34] using Leica Application Suite AF software which calculated Pearson's correlation coefficient, overlap coefficient and colocalization rate (colocalization area divided by foreground area) for each pair of images. For both signals the intensity threshold value was set at 40%, and 20% background subtraction was applied. The analysis was performed in two single-plane confocal images acquired from the lamella of one cell; at least 40 cells from three independent experiments were analyzed for each variant.

2.7. Cell fractionation

U937 cells were treated with 20 nM GST-lysenin WT or 200 nM GST-lysenin W20A for 20 min at 4 °C. To activate FcγRIIA, cells were exposed to anti-FcγRIIA (mouse IgG2b, clone IV.3) conjugated with biotin and followed by goat anti-mouse IgG (Sigma). In cells treated with IV.3-biotin alone, FcγRIIA remained non-activated [10,16]. For fractionation, cells (5×10^6) were lysed in the presence of 0.2% Triton X-100 and subjected to ultracentrifugation in 0–40% OptiPrep density gradient [35]. Gradient fractions were analyzed by SDS-PAGE (4–15%) and immunoblotting using rabbit IgG against the GST tag (Sigma), Lyn kinase (Santa Cruz Biotechnology) and NTAL (kindly provided by Dr. V. Horejsi, Prague), all followed by goat anti-rabbit IgG-peroxidase (ICN). To detect the biotin-labeled anti-FcγRIIA antibody, goat anti-biotin IgG-peroxidase (Sigma) was applied. Immunoreactive bands were detected with SuperSignal West Pico chemiluminescent substrate (Pierce).

3. Results

3.1. Surface plasmon resonance analysis of GST-lysenin WT and GST-lysenin W20A interaction with sphingomyelin

To investigate the mode of lysenin interaction with sphingomyelin in membranes, we performed surface plasmon resonance analysis on liposomes composed of sphingomyelin mixed either with DOPC or DPPC (molar ratio 1:1). Such lipid composition was expected to induce heterogeneous or homogenous sphingomyelin distribution in the plane of the membrane, respectively [36–39]. GST-lysenin WT bound strongly to the SM/DOPC liposomes as indicated by the resonance value of about 5300 RU after 5 min of dissociation (600 s from the beginning of the measurements) (Fig. 1A). The dissociation phase which started at 300 s with washing of samples with a buffer showed the amount of the protein stably associated with the liposomes and was taken into consideration when comparing the binding of lysenin to liposomes of various composition. The binding of GST-lysenin WT to SM/DOPC liposomes was approximately twice as strong as the binding to the SM/DPPC ones. GST-lysenin WT failed to bind to DOPC or DPPC alone, pointing to the specificity of the protein toward sphingomyelin (Fig. 1A). As lysenin interaction with sphingomyelin is likely to involve the conserved tryptophan residues of the protein [23], we examined the membrane interaction of GST-lysenin W20A. The mutant lysenin bound more weakly to sphingomyelin-containing liposomes than did WT lysenin, however, it still preferred sphingomyelin-containing membranes over those containing DOPC or DPPC alone (Fig. 1B). In contrast to lysenin WT, the mutant protein did not display a significant difference in the binding to sphingomyelin mixed with DOPC or DPPC (Fig. 1B).

The influence of sphingomyelin clustering on the binding of lysenin was further examined after supplementation of SM/DPPC liposomes with cholesterol (molar ratio 1:1:1), as cholesterol was likely to facilitate the formation of sphingomyelin-rich domains in this lipid mixture [25,40]. Under these conditions the amount of GST-lysenin WT bound to the membrane was significantly increased (approximately ~6000 versus ~2000 RU after 5 min of dissociation, in the presence and absence of cholesterol, respectively). As a result, the binding of GST-lysenin WT to SM/DPPC/cholesterol liposomes approached the maximum level found for the SM/DOPC/cholesterol and SM/DOPC liposomes (Fig. 1A). Incorporation of cholesterol to sphingomyelin-containing liposomes also improved the binding of GST-lysenin W20A. The effect of cholesterol on the mutant lysenin binding was similar for SM/DOPC and SM/DPPC membranes (Fig. 1B). In contrast, addition of cholesterol to liposomes containing DOPC or DPPC (at a molar ratio of 1:1 to PC) made the binding of GST-lysenin WT and W20A the weakest among all liposomes tested (Fig. 1A and B). GST alone did not bind to any liposomes

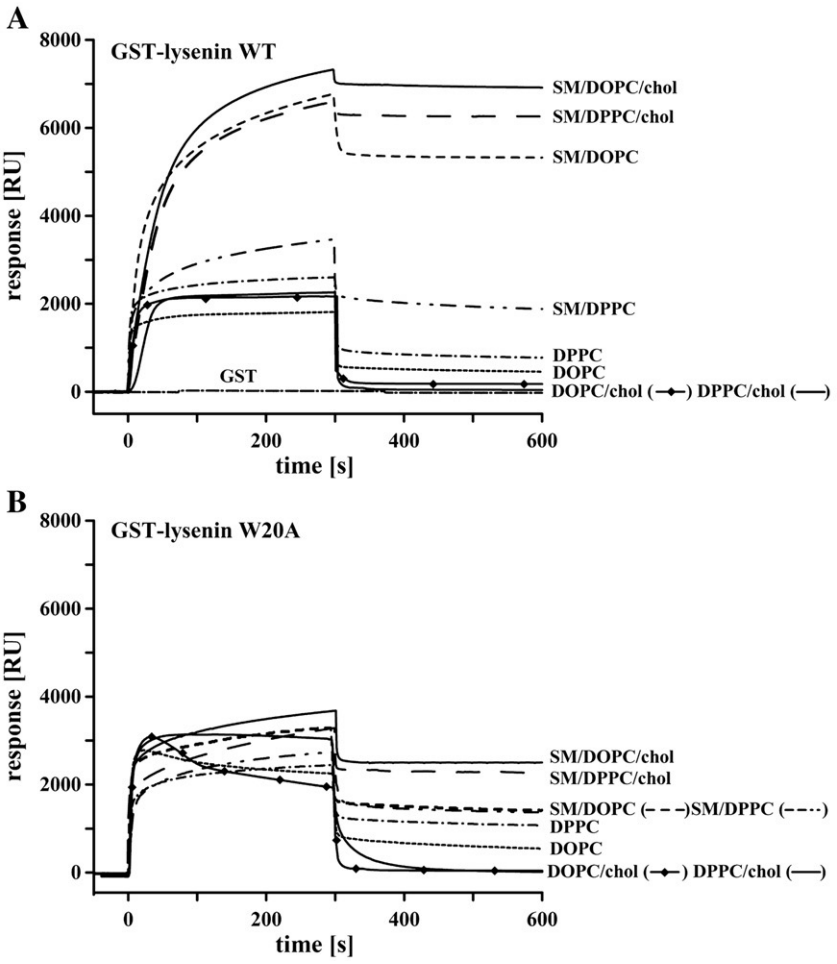

Fig. 1. Lysenin binding to liposomes of various lipid compositions. The following lipid mixtures were used: SM/DOPC or SM/DPPC (molar ratio 1:1) with or without cholesterol in equimolar amounts to SM, DOPC/cholesterol or DPPC/cholesterol (molar ratio 1:1) and DOPC or DPPC alone. SPR sensograms of GST-lysenin WT (A) and the mutant GST-lysenin W20A (B) binding to liposomes immobilized on the surface of sensor chip L1. Proteins (2 μM) were injected at a flow rate of 30 μl/min in 150 mM NaCl, 30 mM Tris, pH 8.0. In (A) a sensogram of GST (2 μM) binding to SM/DOPC/cholesterol liposomes is also seen. Typical sensograms from three or four independent experiments are presented.

used (Fig. 1A and data not shown), indicating that the tag did not affect the interaction of GST-lysenin WT and W20A with the membranes.

3.2. Atomic force microscopy studies of sphingomyelin-containing monolayers

For analysis of the topography of monolayers of various lipid compositions, the monolayers were transferred to the mica-stearic acid support and examined by atomic force microscopy. The studies revealed phase separation in SM/DOPC but not in SM/DPPC membranes (molar ratio 3:7; Fig. 2A and C). The SM/DPPC membrane was flat and essentially featureless (Fig. 2C), which is in agreement with earlier data on miscibility of C16:0 sphingomyelin and DPPC obtained by differential scanning calorimetry [36]. In contrast, in images of SM/DOPC membranes interspersed small and large domains (0.1–1 μm in diameter) raised above the surrounding monolayer were seen (Fig. 2A, lighter areas). These distinct areas can correspond to sphingomyelin-rich domains as suggested earlier [37,38]. Membranes of SM/DOPC/cholesterol (molar ratio 3:7:3) had an appearance resembling that of membranes without cholesterol (Fig. 2B). In contrast, SM/DPPC membranes supplemented with cholesterol underwent reorganization, displayed numerous dispersed raised islands 0.1–0.4 μm in diameter (Fig. 2D), indicating that at these conditions phase separation occurred.

3.3. GST-lysenin W20A binds sphingomyelin but lacks lytic activity

As the binding of GST-lysenin WT to sphingomyelin-containing membranes coincides with protein oligomerization and membrane permeation [26,28], we performed experiments with release of carboxyfluorescein from liposomes of various lipid composition. We found that GST-lysenin WT released carboxyfluorescein 1.9-fold more effectively from SM/DOPC liposomes than from SM/DPPC ones, as estimated after 10 min of the dye efflux (molar ratio of SM to DOPC or DPPC was 3:7). Supplementation of the liposomes with cholesterol in ratio equimolar to SM led to an increase in the level of permeabilization by about 1.4-fold from SM/DOPC and about 2.4-fold from SM/DPPC liposomes (Fig. 3). The data on the permeabilizing activity of GST-lysenin WT were in agreement with the SPR studies on the binding of the proteins to various liposomes (Fig. 1A). GST-lysenin W20A did not induce release of carboxyfluorescein from liposomes regardless of their lipid composition (Fig. 3). The loss of permeabilizing activity of GST-lysenin W20A correlated with its inability to form SDS-resistant oligomers (Fig. 3). It has to be emphasized that the mutant lysenin did bind to membranes in a sphingomyelin-dependent manner, albeit less strongly than did lysenin WT (see Fig. 1B). The protein–lipid overlay assay which relied on binding of lysenin to lipids deposited onto nitrocellulose [28] confirmed that the binding of GST-lysenin W20A to sphingomyelin was about 8-fold weaker than that of GST-lysenin WT (not shown).

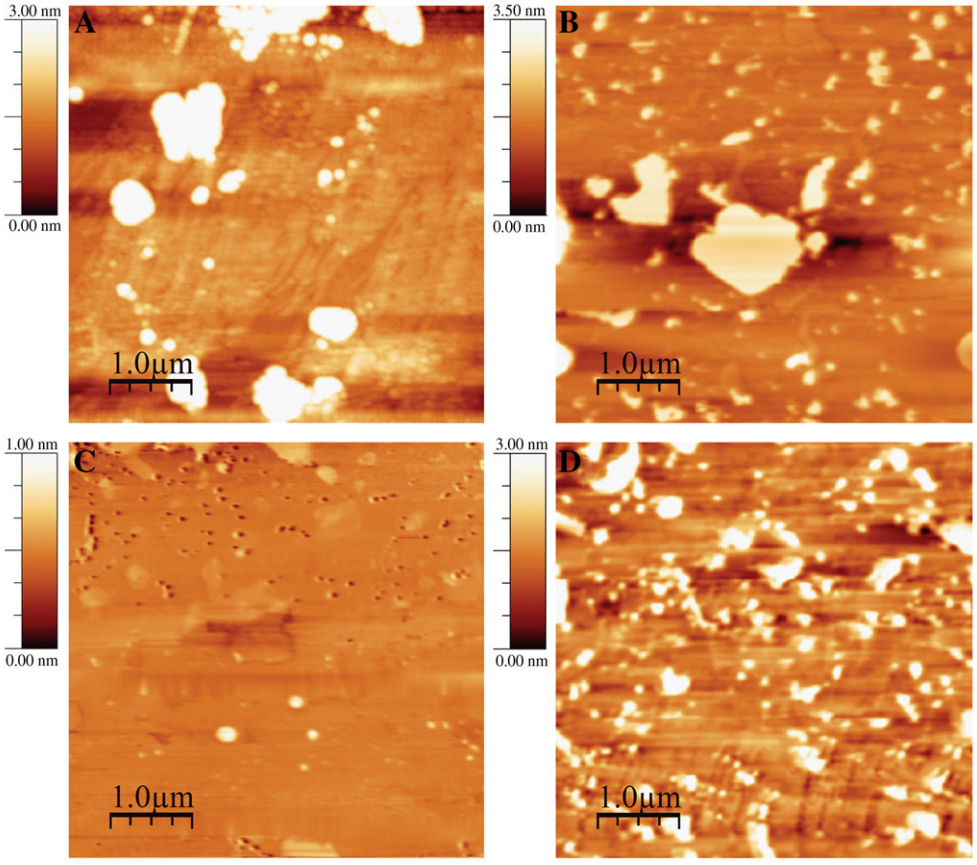

Fig. 2. AFM images of membranes of different composition. (A) SM/DOPC (molar ratio 3:7), (B) SM/DOPC/cholesterol (molar ratio 3:7:3), (C) SM/DPPC (molar ratio 3:7) and (D) SM/DPPC/cholesterol (molar ratio 3:7:3) membranes. For imaging, monolayers were deposited on mica-stearic acid support at surface pressure of 21 mN/m.

3.4. W20A mutation affects surface activity of lysenin

To further study the interactions of GST-lysenin WT and W20A with model membranes, monomolecular surface pressure experiments were undertaken, starting with an analysis of spontaneous adsorption of the protein at the argon–water interface. Injection of GST-lysenin WT into the aqueous sub-phase led to an increase of surface pressure in a dose-dependent manner (Fig. 4A), as a result of the surface-active properties of lysenin molecules. At low protein concentrations (0.2–2.0 nM) a pronounce lag phase in the surface pressure changes was observed. The cooperative character of the changes suggests that GST-lysenin WT undergoes self-aggregation in solution. The lag phase became shorter with increasing protein concentrations and was no longer detectable at 30 nM GST-lysenin WT.

GST-lysenin W20A was also surface-active and induced changes of the surface pressure in a dose-dependent manner (Fig. 4B). Analysis of the adsorption kinetics of GST-lysenin W20A showed that the rates of

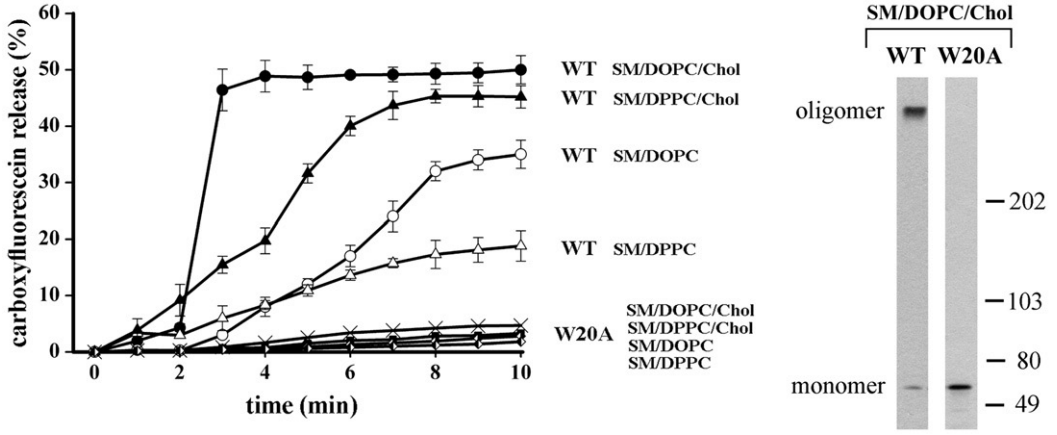

Fig. 3. Lytic activity of lysenin correlates with its oligomerization. Carboxyfluorescein release from LUV composed of SM/DOPC, SM/DPPC (molar ratio 3:7) containing cholesterol in ratio equimolar to sphingomyelin, when indicated. To induce dye efflux, at time = 0, 100 nM GST-lysenin WT or W20A was added to LUV suspension (1 mM total phospholipid concentration), and the fluorescence was monitored (25 °C). The data are expressed as percentage of the total amount of carboxyfluorescein released from LUV by 0.1% Triton X-100 (mean ± SEM from three measurements). (Right panel) Pelleted SM/DPPC/cholesterol liposomes were subjected to SDS-PAGE and analyzed for the presence of lysenin oligomer and monomer by immunoblotting using rabbit anti-GST and anti-rabbit IgG-peroxidase. Molecular weight standard positions (kDa) shown on the right.

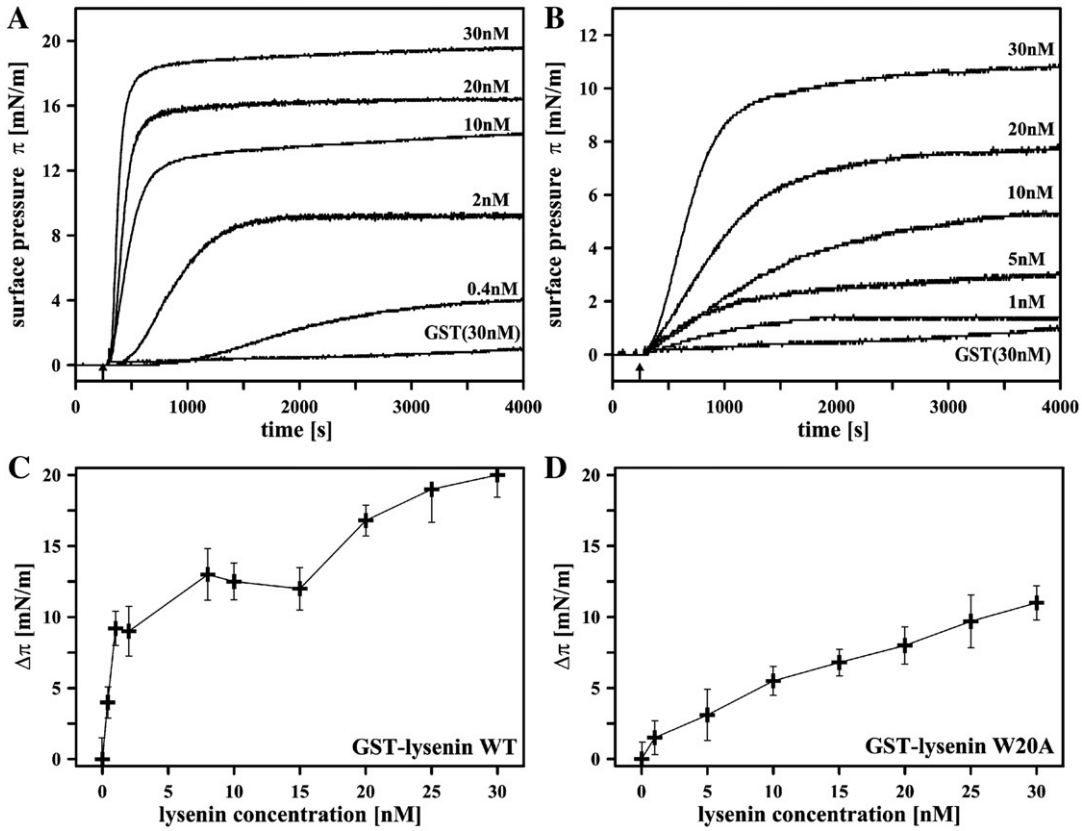

Fig. 4. Adsorption of lysenin at the argon-water interface. (A, B) Kinetics of surface pressure changes caused by various concentrations of GST-lysenin WT (A) and W20A (B). Time of protein injection to water sub-phase is marked with arrow. Plots shown are representative of three independent measurements. (C, D) Maximum increase ($\Delta\pi$) in lateral pressure caused by lysenin adsorption at the argon-water interface as a function of concentration of GST-lysenin WT (C) and GST-lysenin W20A (D) in the water sub-phase. The data are mean ± SEM from three experiments.

the surface pressure changes were comparable to those observed for GST-lysenin WT but the saturation level of surface pressure was substantially lower for the mutant lysenin. Additionally, the sigmoidal shape of the surface pressure time dependences, observed for GST-lysenin WT, did not obey in the case of GST-lysenin W20A, even at the lowest protein concentration.

Fig. 4C and D summarizes the maximal change in surface pressure ($\Delta\pi$) as a function of lysenin concentration. For GST-lysenin WT, the concentration dependence of $\Delta\pi$ displayed two saturation levels: at about 12.5 mN/m and at about 20 mN/m. The data suggest that at the protein concentrations above 15 nM the self-aggregation takes place; the aggregated protein can affect $\Delta\pi$ more effectively than the non-assembled protein. In contrast, for GST-lysenin W20A the maximum change in surface pressure ($\Delta\pi$) increased proportionally to the concentration of the protein in the sub-phase and did not reach a plateau in the investigated concentration range (Fig. 4D). Presumably, the W20A mutation precludes the self-aggregation of lysenin. These observations indicate also that the presence of the GST tag does not determine abilities of GST-lysenin WT and W20A for oligomerization. This notion is important in view of data that GST, naturally dimeric [41], can evoked dimerization of fusion proteins containing this tag [42,43], although other data are also available [44].

Fig. 5 shows changes in the surface pressure of mixed lipid monomolecular layers spread at the argon-water interface, following injection of 30 nM WT or W20A lysenin into the buffer sub-phase. The binding of the proteins to the membranes was analyzed in terms of the two-exponential dependency (Eq. (1)) reflecting the existence of two phases of the process: the fast one characterized by the rate constant α, and the slow one described by the rate constant β (Table 1). The rate constants α and β of the binding of WT lysenin to the mixed SM/DOPC/cholesterol monolayers (molar ratio 3:7:3) were found to be

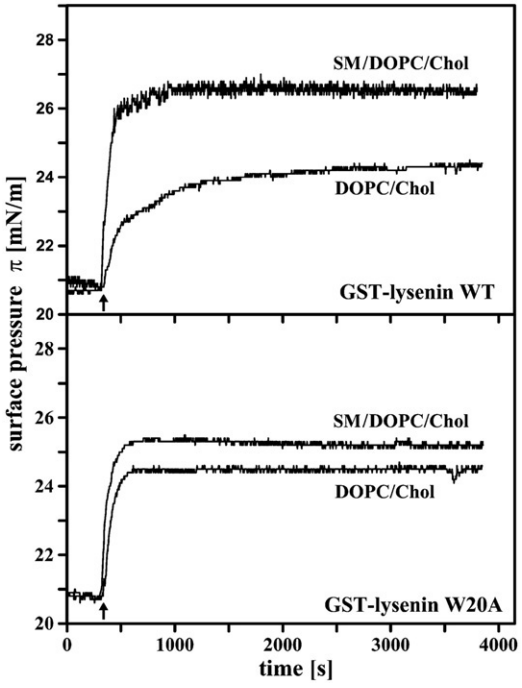

Fig. 5. Insertion of lysenin WT and W20A in lipid monolayers. Kinetics of surface pressure increase caused by penetration of GST-lysenin WT (top panel) and GST-lysenin W20A (lower panel) into the DOPC/cholesterol monolayer spread at the argon–water interface in the absence or presence of sphingomyelin. Monolayers contained SM/DOPC/cholesterol in 3:7:3 molar ratio or DOPC/cholesterol in 7:3 molar ratio. Time of protein injection (30 nM) into water phase beneath the monomolecular layer at the surface pressure of 21 mN/m is marked with arrow. Plots shown represent one of three experiments.

Table 1
Kinetic analysis of lysenin insertion into lipid monolayers.

Lysenin form	Lipid monolayer	α ($\times 10^3$ s^{-1})	α (%)	β ($\times 10^3$ s^{-1})	β (%)	Q ($\times 10^3$ s^{-1})	$\Delta\pi$ (mN/m)
WT	SM/DOPC/CHOL	15.8 ± 1.1	84	3.8 ± 0.9	16	13.8 ± 1.0	5.6 ± 0.2
WT	DOPC/CHOL	11.0 ± 0.8	57	1.2 ± 0.2	43	5.7 ± 0.8	3.7 ± 0.1
W20A	SM/DOPC/CHOL	15.3 ± 1.4	95	0.2 ± 0.1	5	14.5 ± 0.8	5.0 ± 0.2
W20A	DOPC/CHOL	12.0 ± 1.2	94	0.01 ± 0.008	6	11.3 ± 0.5	3.9 ± 0.1

The following lipid mixtures were used: SM/DOPC/cholesterol (molar ratio 3:7:3) or DOPC/cholesterol (molar ratio 7:3). Total phospholipid concentration was 1 mM. The kinetic parameters were derived from experimental data on the change of surface pressure of monolayers as a function of time after injection of 30 nM GST-lysenin WT or W20A into water sub-phase (see Fig. 5) and fitted to a two-exponential equation (Eq. (2)). α and β—rate constants of the fast and slow phases of protein adsorption at the interface; percentage contribution of the rates was calculated on the basis of the pre-exponential factors; Q—average rate constant; $\Delta\pi$—total surface pressure change: difference between membrane surface pressure at plateau and at the moment of injection of the protein into water sub-phase. Data shown mean ± SEM from three experiments.

15.8×10^{-3} s^{-1} (84%) and 3.8×10^{-3} s^{-1} (16%), respectively. The maximum increase in the surface pressure of the monolayer, $\Delta\pi$, was as high as 5.6 mN/m. The insertion of GST-lysenin WT into the DOPC/cholesterol (molar ratio 7:3) membrane devoid of sphingomyelin was less effective and yielded a $\Delta\pi$ of 3.7 mN/m. The lack of sphingomyelin in the system resulted in a pronounced decrease in both the α and β rate constants (Table 1). At these conditions the contribution of the slow β component in the binding increased at the expense of the fast α component and, therefore, the average rate representing the relative binding efficiency Q (Eq. (2)) of GST-lysenin WT dropped from 13.8×10^{-3} s^{-1} in the case of sphingomyelin-containing membranes to 5.7×10^{-3} s^{-1} in the case of the sphingomyelin-lacking system (Table 1). The presence of sphingomyelin in monolayers also affected the insertion of GST-lysenin W20A. The surface pressure changes ($\Delta\pi$) of the monolayer evoked by GST-lysenin W20A reached 5 mN/m with sphingomyelin and 3.9 mN/m without sphingomyelin (Table 1). The decreased range of the surface pressure changes was accompanied by decreased rate constants α and β of the binding of GST-lysenin W20A to DOPC/cholesterol monolayer. It should be noted that in the case of GST-lysenin W20A the fast rate constant (α) of the protein adsorption to a sphingomyelin-containing membrane contributed to the protein insertion to a higher degree (95%) than it did for GST-lysenin WT (84%) (Table 1). This difference can reflect a different organization of the WT and W20A lysenin molecules in the sphingomyelin-containing membranes.

3.5. Detergent-resistant membrane fragments are targets for GST-lysenin WT

We examined whether the preferential interaction of GST-lysenin WT with sphingomyelin clusters would also be reflected in its binding to various domains of the plasma membrane. To separate detergent-resistant and detergent-soluble fractions of the plasma membrane, 0.2% Triton X-100 lysates of U937 monocytes were subjected to density gradient ultracentrifugation. A line of previous data indicated that the detergent-resistant membranes isolated at these conditions in buoyant fractions 1–2 of the gradient are derived from rafts which serve as sites of accumulation of activated immunoreceptor FcγIIA and signal generation [10,16,18]. We found that GST-lysenin WT incubated with cells prior to lysis was recovered mainly in the low density fractions 1–2 of the gradient (Fig. 6). Only oligomers over 350 kDa, probably corresponding to lysenin hexamers, were detected. Fractions 1–2 of the gradient also contained a distinct pool of Lyn kinase and NTAL adaptor protein, two markers of rafts. On the other hand, fractionation of lysates of cells preincubated with GST-lysenin W20A revealed that the mutant lysenin was found only as monomers of about 63 kDa in fractions 6–7 of high density where Triton X-100-soluble proteins were located (Fig. 6). Activation of FcγRIIA led to a shift of the receptor from the high-density fractions 5–7 towards fractions 1–2 of density gradients (Fig. 6).

To follow the dynamics of sphingomyelin in the plasma membrane we labeled with lysenin the surface of resting cells and cells after FcγRIIA activation (Fig. 7). In resting cells FcγRIIA was uniformly distributed over the cell surface while GST-lysenin WT formed numerous tiny clusters as revealed by three-dimensional analysis of the distribution of intensity of fluorescence attributed to the receptor and to lysenin (Fig. 7A and A'). The GST-lysenin WT fluorescence dots were dispersed across the membrane with distinct labeling of cell edges (Fig. 7A'). Activation of FcγRIIA led to a prominent receptor clustering in the plane of the plasma membrane (Fig. 7C), confirming earlier reports [10,45]. Surprisingly, at those conditions we detected simultaneous clustering of the sphingomyelin label (Fig. 7C'). However, in contrast to the distinct spikes of fluorescence attributed to the receptor, sphingomyelin decoration by GST-lysenin WT was often observed as dense assemblies of 3–5 adjacent fluorescence peaks (Fig. 7C and C', lower panel). GST-lysenin W20A stained the cell surface diffusively and formed crude intense dots concentrated over

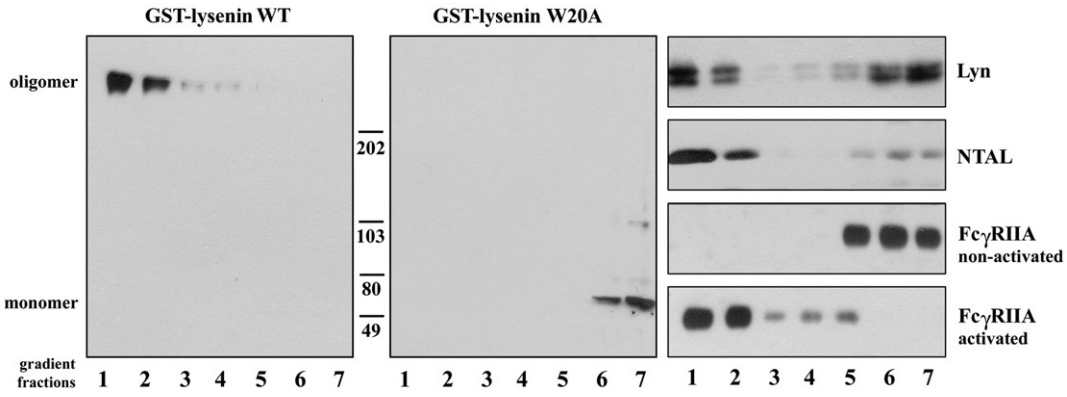

Fig. 6. GST-lysenin WT but not GST-lysenin W20A is present in DRM fractions. U937 monocytes were incubated with 20 nM GST-lysenin WT or with 200 nM GST-lysenin W20A, lysed in 0.2% Triton X-100, fractionated over density gradients and analyzed for the distribution of GST-lysenin WT and GST-lysenin W20A revealed by the GST tag, and for Lyn kinase and NTAL adaptor protein as two raft markers. In a series of experiments living cells were treated either with mouse IgG anti-FcγRIIA labeled with biotin (receptor non-activated) or with the anti-FcγRIIA IgG-biotin and goat anti-mouse IgG (receptor activated). Distribution of FcγRIIA in gradient fractions was revealed with anti-biotin IgG. Molecular weight standard positions are shown between gels in kDa.

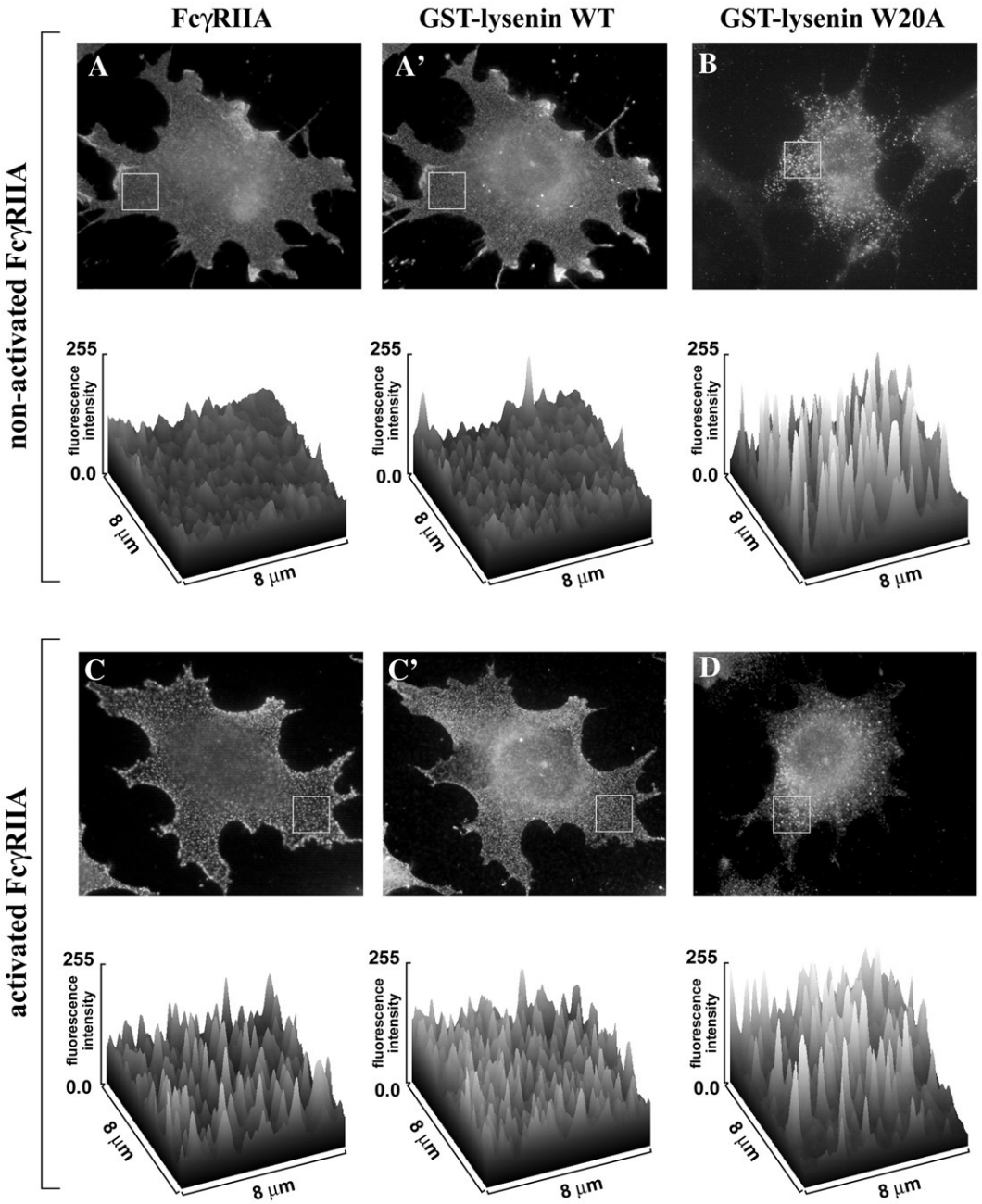

Fig. 7. Activation of FcγRIIA induces redistribution of plasma membrane sphingomyelin decorated with GST-lysenin WT but not with GST-lysenin W20A. Cells were either exposed to IV.3 anti-FcγRIIA mouse IgG and fixed (non-activated FcγRIIA, upper panel) or incubated with the IV.3 anti-FcγRIIA mouse IgG followed by goat anti-mouse IgG-Texas Red prior to fixation (activated FcγRIIA, lower panel). The fixed cells were subsequently incubated either with 20 nM GST-lysenin WT (A, A' and C, C') or 200 nM GST-lysenin W20A (B, D) followed by rabbit anti-lysenin IgG and goat anti-rabbit IgG-FITC. After examination under a fluorescent microscope, distribution and intensity of fluorescence signals attributed to FcγRIIA (A, C), GST-lysenin WT (A', C') and GST-lysenin W20A (B, D) were analyzed in marked areas of the plasma membrane (8×8 μm) and displayed as three-dimensional maps shown at the bottom of corresponding cell images. Data representative for two experiments are shown.

the cell body. The distribution of the GST-lysenin W20A label was not affected by activation of FcγRIIA (Fig. 7B and D).

To estimate possible colocalization of lysenin with activated FcγRIIA a quantitative analysis was performed of dual-color confocal images of either GST-lysenin WT or GST-lysenin W20 and the receptor (Supplementary Fig. 1 online). For that, three different quantities were calculated (Table 2), starting with the Pearson's correlation coefficient which provides information about the similarity of shape between two images without regard to the average intensity of the signals [34]. The value for co-immunostaining of GST-lysenin W20A and activated FcγRIIA was very low (about 0.22 in relation to 1 as the maximal value), while for GST-lysenin WT and the receptor it reached 0.32 (Table 2). The overlap coefficient had higher values than those of the Pearson's correlation (Table 2). However, this parameter is strongly affected by differences in the fluorescence patterns between the compared images [34]. Finally, a lack of co-localization of GST-lysenin W20A and FcγRIIA and moderate co-localization of WT lysenin and the receptor was indicated by the colocalization rate calculated as the percentage of area where the two fluorescences coincided. For comparison, the Pearson's correlation coefficient and the overlap coefficient calculated for tyrosine-phosphorylated proteins and activated FcγRIIA were as high as 0.67–0.81 and the colocalization rate of the two signals reached 76% (Table 2), which is in agreement with previous observations [10]. As labeling of tyrosine-

Table 2
Quantification of colocalization of GST-lysenin WT and GST-lysenin W20A with activated FcγRIIA.

Co-immunostaining	Pearson's correlation	Overlap coefficient	Colocalization rate
GST-lysenin WT/activated FcγRIIA (no detergent)	0.32 ± 0.01	0.59 ± 0.03	43.44% ± 1.60%
GST-lysenin WT/activated FcγRIIA (digitonin-treated)	0.45 ± 0.01	0.60 ± 0.01	49.66% ± 1.28%
GST-lysenin WT/activated FcγRIIA (TX-treated)	0.44 ± 0.02	0.56 ± 0.02	45.31% ± 0.81%
GST-lysenin W20/activated FcγRIIA (no detergent)	0.22 ± 0.01	0.49 ± 0.01	25.21% ± 1.88%
PY-proteins/activated FcγRIIA (digitonin-treated)	0.78 ± 0.01	0.81 ± 0.05	76.56% ± 1.76%
PY-proteins/activated FcγRIIA (TX-treated)	0.67 ± 0.03	0.75 ± 0.02	69.35% ± 2.06%

For comparison, colocalization of tyrosine-phosphorylated proteins (PY-proteins) with the receptor was estimated. To activate FcγRIIA, cell were exposed to IV.3 anti-FcγRIIA mouse IgG and goat anti-mouse IgG-Texas Red. After fixation, the cells were incubated with GST-lysenin WT or W20A followed by rabbit anti-lysenin IgG and goat anti-rabbit IgG-FITC (no detergent treatment). In a series of experiments, cells after fixation but prior to lysenin binding were treated either with 0.05% Triton X-100 or 0.005% digitonin. When tyrosine-phosphorylated proteins were analyzed, cell after activation of FcγRIIA were fixed, treated either with 0.05% Triton X-100 or 0.005% digitonin and labeled with rabbit anti-phosphotyrosine followed by goat anti-rabbit IgG conjugated with FITC. Colocalization of proteins was analyzed in images of 40 cells from three independent experiments for each variant. Data shown are mean ± SEM.

phosphorylated proteins required permeabilization of cells with 0.005% digitonin or 0.05% Triton X-100, colocalization of GST-lysenin WT and activated FcγRIIA was also estimated at these conditions (Table 2). It was found that both detergents promote colocalization of lysenin WT and activated receptor, as reflected by an increase in the Pearson's correlation values for the two proteins in permeabilized cells (Table 2).

4. Discussion

The interest in distribution of sphingolipids in membranes has been increasing with the discovery of sphingolipid/cholesterol microdomains in the plasma membrane and their postulated involvement in various cellular functions, including signal transduction. Studies on raft structure and function have drawn attention to protein probes of cholesterol and sphingomyelin, with lysenin as an example of the latter [30].

In this report we demonstrated that lysenin WT recognized sphingomyelin present in a detergent-resistant fraction of the plasma membrane that was attributed to rafts. In contrast, the W20A mutant lysenin was absent from this fraction and occupied fractions of high density in which detergent-soluble components of the plasma membrane were recovered. The data are in line with the results of SPR studies performed on model membranes showing that high amounts of lysenin WT bound to SM/DOPC, SM/DOPC/cholesterol and SM/DPPC/cholesterol but not SM/DPPC liposomes, thus pointing to the importance of phase separation of sphingomyelin in the plane of the membrane for the protein binding. Lysenin W20A has apparently lost the ability of preferential interaction with sphingomyelin-rich clusters, as it bound in similar amounts to liposomes containing sphingomyelin mixed with DOPC and DPPC. Mixtures of sphingomyelin with DOPC or DPPC have been used previously to force homo- or heterogeneous distribution of sphingomyelin in membranes. It was shown by differential scanning calorimetry that semi-synthetic brain C16:0 sphingomyelin was fully miscible with DPPC at all the ratios studied [36]. Accordingly, we used a mixture of the semi-synthetic brain C16:0 sphingomyelin with DPPC (molar ratios 1:1 and 3:7) to prepare membranes with homogenous sphingomyelin distribution. AFM studies confirmed uniform lipid distribution in the obtained SM/DPPC (molar ratio 3:7) membrane (Fig. 2C). In contrast, in the mixture with DOPC, C16:0 sphingomyelin separated in the plane of the plasma membrane forming a heterogeneous population of small and large domains (Fig. 2A, SM/DOPC at molar ratio 3:7). Although not exactly matching, this lipid mixture can correspond to a mixture of egg PC (PC containing saturated and unsaturated fatty acyl chains, according to Avanti data) with brain sphingomyelin at above 33 mol%. Separation of gel phase sphingomyelin from the PC-rich liquid crystalline phase was detected in membranes of such lipid composition at 20 °C [46]. Furthermore, separation of sphingomyelin-rich and DOPC-rich phases was well documented by AFM analysis of membranes with a higher content of brain or C16:0 sphingomyelin (SM/DOPC at molar ratio 1:1) [37–39]. Those conditions correspond to these of our SPR studies.

After supplementation of an SM/DOPC mixture with cholesterol, sphingomyelin formed a liquid-ordered phase that still co-existed with the liquid-disordered phase in the membrane, as shown by spectroscopic studies [47]. Addition of cholesterol to C16:0 SM/DOPC in the range of 10–50 mol% has been reported to induce a progressive increase of the size of the sphingomyelin-rich domains visualized by AFM [37,38]. In our hands, enrichment of SM/DOPC liposomes with cholesterol (molar ratio 1:1:1) only moderately increased the amounts of lysenin WT bound to liposomes (Fig. 1A) and did not change substantially the appearance of SM/DOPC membrane in AFM (SM/DOPC/cholesterol at molar ratio 3:7:3; Fig. 2A and B). In contrast, cholesterol added to a mixture of SM and DPPC markedly facilitated the binding of lysenin WT to liposomes (Fig. 1A). Of note, cholesterol concomitantly induced a shift from a homo- to a heterogenous distribution of sphingomyelin in SM/DPPC membranes [Fig. 2C and D, and 25,40]. The data showing facilitated binding of lysenin WT to SM/DPPC/cholesterol membranes are in agreement with other reports showing that lysenin WT is prone to binding sphingomyelin separated from PC into domains in membranes [25]. It is of note that cholesterol has also been shown to facilitate lysenin WT oligomerization by increasing fluidity of sphingomyelin-containing membranes [27]. This effect, in addition to phase separation, can contribute to the increase of the amount of lysenin WT bound to cholesterol-containing liposomes on the BIAcore sensor and the significant release of carboxyfluorescein from liposomes (Fig. 1A, Fig. 3). The mutant GST-lysenin W20A did not discriminate in its binding between sphingomyelin mixed with DOPC or DPPC, regardless of cholesterol presence (Fig. 1B).

The loss of the preference of GST-lysenin W20A to bind sphingomyelin microdomains correlated with an inability of the mutant protein to oligomerize and the parallel loss of the lytic activity. SPR analysis indicated that less GST-lysenin W20A remained bound to sphingomyelin-containing liposomes in comparison with GST-lysenin WT. The weaker interaction of GST-lysenin W20A with sphingomyelin was confirmed by the protein/lipid overlay and liposome binding assays (not shown). Furthermore, the surface pressure changes induced by lysenin W20A both at the argon–water interface and in sphingomyelin-containing monolayers were lower than those induced by the same concentrations of lysenin WT. The data indicate that the mutant lysenin is more hydrophilic, with a limited ability to penetrate the hydrophobic region of membranes. Measurements of the surface pressure changes of a monomolecular layer showed that upon binding to sphingomyelin-containing membrane, GST-lysenin WT and W20A share a common fast phase of the process described by the rate constant α (Table 1). The lack of the slow phase β in the binding of GST-lysenin W20A probably reflects the inability of the protein to insert and form stable hexamers in the membrane. All the data suggest that formation of stable oligomers by lysenin WT enhances its binding to sphingomyelin clusters in a positive feedback

manner. The inability to oligomerize can account for the weak interaction of GST-lysenin W20A with sphingomyelin clusters. Formation of stably oligomers in sphingomyelin-containing membranes by lysenin WT correlates with self-assembly of the protein into trimers even in the absence of the lipid [31]. Accordingly, self-association of GST-lysenin WT, but not lysenin GST-lysenin W20A, is suggested by the sigmoidal shape of the plots of surface pressure versus time recorded for lysenin WT only.

Studies of lysenin W20A provide new information on the organization of lysenin WT oligomers in membranes. A prediction of the secondary structure of lysenin suggested the existence of an α-helix encompassing residues G256-T267 and two possible α-helices located in the middle and at the N-terminus of the protein [24]. Linear dichroism measurements showed that the C-terminal α-helix can penetrate lipid bilayers [31]. Deletion of the C-terminal fragment starting from amino acid 247 abolished the binding of lysenin to sphingomyelin [30]. A similar effect was exerted by mutation of any of the W116, W187, W245 or W291 residues [23]. Based on these data we suggest that the C-terminal α-helix, in cooperation with the indicated tryptophan residues, becomes embedded in the membrane. However, these interactions are not sufficient to stably anchor the protein in the membrane judging from the weak binding of GST-lysenin W20A. The irreversible binding of lysenin requires an involvement of the N-terminus which governs the protein oligomerization and concomitant formation of a membrane pore. Presumably also the N-terminus becomes inserted into the membrane. The W20A mutation as well as truncation of the N-terminal 60 amino acid residues disable the second stage of the lysenin–sphingomyelin interaction and suppress the lytic activity of lysenin [28,30]. Antibodies directed against distinct C- or N-terminal regions of lysenin did not recognize oligomers of lysenin WT, supporting the suggestion that those protein fragments are buried in the membrane [22]. Large, SDS-sensitive conglomerates of lysenin W20A revealed by native electrophoresis in sphingomyelin-containing membranes [28] indicate that the mutant forms aggregates different from the small, regular assemblies composed of six monomers of lysenin WT. The conglomerates of mutant lysenin probably do not penetrate the membrane, as indicated by the lack of the channel and lytic activities of the protein [28 and this report].

When applied to detect sphingomyelin on the cell surface, GST lysenin WT and W20A displayed different patterns of staining, with large aggregates observed for the mutant lysenin only. Concomitantly, lysenin WT and W20A were recovered in detergent-resistant and detergent-soluble fractions of the plasma membrane, respectively. The exclusive partitioning of GST-lysenin WT to the membrane fractions believed to originate from rafts is in line with the results of studies on the interaction of GST-lysenin WT with sphingomyelin clusters in model membranes discussed above. Rafts serve as signaling platforms for the immunoreceptor FcγRIIA [10,16]. The receptor associates with the rafts upon activation, which is reflected by its shift from high to low density fractions where it co-exists with signaling proteins like Lyn kinase and NTAL as well as with oligomers of GST-lysenin WT. However, when visualized in intact cells, activated FcγRIIA colocalized moderately with lysenin WT oligomers (Supplementary Fig. 1 online and Table 2). Such separation can ensue from steric hindrance imposed on the lysenin-sphingomyelin interaction by gangliosides occupying the rafts [30]. On the other hand, lysenin can selectively bind to sphingomyelin located at the edges of rafts, where defects in lipid packing favor protein–lipid interactions. It has been suggested that such defects in lipid packing increase the accessibility of sphingomyelin to equinatoxin II, another sphingomyelin-specific pore-forming protein toxin originating from *Actinia equina* [21,48,49]. A similar mechanism was proposed to govern the interaction of PLA_2 and glicerophospholipids in the course of the action of the enzyme [50], pointing to the lipid-phase boundaries as sites of binding of water-soluble proteins with their lipid targets [51].

Despite the separated decorations of FcγRIIA and sphingomyelin, the receptor- and sphingomyelin-rich domains seem to be functionally related since receptor activation affected sphingomyelin distribution as revealed by GST-lysenin WT (Fig. 7). We assume that the inability of GST-lysenin W20A to oligomerize affects its interaction with sphingomyelin in the plasma membrane. The weak binding of the mutant lysenin to sphingomyelin can prevent it stably docking in rafts (at their edges); as a result, large "invalid oligomers" of GST-lysenin W20A are formed outside rafts and are recovered in detergent-soluble membrane fractions (Fig. 6). Accordingly, activation of FcγRIIA did not change the pattern of plasma membrane decoration by the W20A mutant lysenin.

Taken together, the presented data suggest that only lysenin WT recognizes raft sphingomyelin where it forms stable oligomers. The mutant lysenin W20A, which does not oligomerize, interacts with another pool of the lipid, the existence of which has been suggested earlier [17,18]. The results shed new light on the data on sphingomyelin distribution in the plasma membrane revealed by monomeric non-toxic lysenin [30].

Acknowledgments

We thank Dr. Andrej Bavdek (Department of Biology, University of Ljubljana, Slovenia) for the introduction to the SPR technique, Dr. V. Horejsi (Institute of Molecular Genetics, Prague, Czech Republic) for providing anti-NTAL antibody and Artur Wolny (Laboratory of Confocal Microscopy, the Nencki Institute of Experimental Biology) for help with image analysis. This work was supported by grants N N301 030234 to A.S. and PBZ/MEiN/01/2006/44 to M.H. from the Ministry of Science and Higher Education, Poland.

Appendix A. Supplementary data

Supplementary data associated with this article can be found, in the online version, at doi:10.1016/j.bbamem.2009.12.004.

References

[1] K. Simons, D. Toomre, Lipid rafts and signal transduction, Nat. Rev. Mol. Cell Biol. 1 (2000) 31–39.
[2] V. Horejsi, Membrane rafts in immunoreceptor signaling: new doubts, new proofs? Trends Immunol. 23 (2002) 562–564.
[3] E.K. Fridriksson, P.A. Shipkova, E.D. Sheets, D. Holowka, B. Baird, F.W. McLafferty, Quantitative analysis of phospholipids in functionally important membrane domains from RBL-2H3 mast cells using tandem high-resolution mass spectrometry, Biochemistry 38 (1999) 8056–8063.
[4] L.J. Pike, X. Han, K.N. Chung, R.W. Gross, Lipid rafts are enriched in arachidonic acid and plasmenylethanolamine and their composition is independent of caveolin-1 expression: a quantitative electrospray ionization/mass spectrometric analysis, Biochemistry 41 (2002) 2075–2088.
[5] A.M. Shenoy-Scaria, L.K. Gauen, J. Kwong, A.S. Shaw, D.M. Lublin, Palmitylation of an amino-terminal cysteine motif of protein tyrosine kinases p56lck and p59fyn mediates interaction with glycosyl-phosphatidylinositol-anchored proteins, Mol. Cell. Biol. 13 (1993) 6385–6392.
[6] K.A. Melkonian, A.G. Ostermeyer, J.Z. Chen, M.G. Roth, D.A. Brown, Role of lipid modifications in targeting proteins to detergent-resistant membrane rafts. Many raft proteins are acylated, while few are prenylated, J. Biol. Chem. 274 (1999) 3910–3917.
[7] X. Liang, A. Nazarian, H. Erdjument-Bromage, W. Bornmann, P. Tempst, M.D. Resh, Heterogeneous fatty acylation of Src family kinases with polyunsaturated fatty acids regulates raft localization and signal transduction, J. Biol. Chem. 76 (2001) 30987–30994.
[8] R.J. Schroeder, S.N. Ahmed, Y. Zhu, E. London, D.A. Brown, Cholesterol and sphingolipid enhance the Triton X-100 insolubility of glycosylphosphatidylinositol-anchored proteins by promoting the formation of detergent-insoluble ordered membrane domains, J. Biol. Chem. 273 (1998) 1150–1157.
[9] E. London, D.A. Brown, Insolubility of lipids in Triton X-100: physical origin and relationship to sphingolipid/cholesterol membrane domains (rafts), Biochim. Biophys. Acta 1508 (2000) 182–195.
[10] K. Kwiatkowska, J. Frey, A. Sobota, Phosphorylation of FcγRIIA is required for the receptor-induced actin rearrangement and capping: the role of membrane rafts, J. Cell. Sci. 116 (2003) 537–550.
[11] D. Holowka, J.A. Gosse, A.T. Hammond, X. Han, P. Sengupta, N.L. Smith, A. Wagenknecht-Wiesner, M. Wu, R.M. Young, B. Baird, Lipid segregation and IgE

receptor signaling: a decade of progress, Biochim. Biophys. Acta 1746 (2005) 252–259.
[12] A. Charruyer, S. Grazide, C. Bezombes, S. Müller, G. Laurent, J.P. Jaffrezou, UV-C light induces raft-associated acid sphingomyelinase and JNK activation and translocation independently on a nuclear signal, J. Biol. Chem. 280 (2005) 19196–19204.
[13] R.N. Kolesnick, F.M. Goni, A. Alonso, Compartmentalization of ceramide signaling: physical foundations and biological effects, J. Cell. Physiol. 184 (2000) 285–300.
[14] H. Grassme, A. Jekle, A. Riehle, H. Schwarz, J. Berger, K. Sandhoff, R. Kolesnick, E. Gulbins, CD95 signaling via ceramide-rich membrane rafts, J. Biol. Chem. 276 (2001) 20589–20596.
[15] H. Grassme, V. Jendrossek, J. Bock, A. Riehle, E. Gulbins, Ceramide-rich membrane rafts mediate CD40 clustering, J. Immunol. 168 (2002) 298–307.
[16] A.B. Abdel Shakor, K. Kwiatkowska, A. Sobota, Cell surface ceramide generation precedes and controls FcγRII clustering and phosphorylation in rafts, J. Biol. Chem. 279 (2004) 36778–36787.
[17] C.M. Linardic, Y.A. Hannun, Identification of a distinct pool of sphingomyelin involved in the sphingomyelin cycle, J. Biol. Chem. 269 (1994) 23530–23537.
[18] M. Korzeniowski, A.B. Shakor, A. Makowska, A. Drzewiecka, A. Bielawska, K. Kwiatkowska, A. Sobota, FcγRII activation induces cell surface ceramide production which participates in the assembly of the receptor signaling complex, Cell. Physiol. Biochem. 20 (2007) 347–356.
[19] S. Lange, F. Nussler, E. Kauschke, G. Lutsch, E.L. Cooper, A. Herrmann, Interaction of earthworm hemolysin with lipid membranes requires sphingolipids, J. Biol. Chem. 272 (1997) 20884–20892.
[20] R. Ishitsuka, S.B. Sato, T. Kobayashi, Imaging lipid rafts, J. Biochem. 137 (2005) 249–254.
[21] P. Schon, A.J. García-Saez, P. Malovrh, K. Bacia, G. Anderluh, P. Schwille, Equinatoxin II permeabilizing activity depends on the presence of sphingomyelin and lipid phase coexistence, Biophys. J. 95 (2008) 691–698.
[22] A. Yamaji, Y. Sekizawa, K. Emoto, H. Sakuraba, K. Inoue, H. Kobayashi, M. Umeda, Lysenin, a novel sphingomyelin-specific binding protein, J. Biol. Chem. 273 (1998) 5300–5306.
[23] E. Kiyokawa, A. Makino, K. Ishii, N. Otsuka, A. Yamaji-Hasegawa, T. Kobayashi, Recognition of sphingomyelin by lysenin and lysenin-related proteins, Biochemistry 43 (2004) 9766–9773.
[24] A.B. Shakor, E.A. Czurylo, A. Sobota, Lysenin, a unique sphingomyelin- binding protein, FEBS Lett. 542 (2003) 1–6.
[25] R. Ishitsuka, A. Yamaji-Hasegawa, A. Makino, Y. Hirabayashi, T. Kobayashi, A lipid-specific toxin reveals heterogeneity of sphingomyelin-containing membranes, Biophys. J. 86 (2004) 296–307.
[26] A. Yamaji-Hasegawa, A. Makino, T. Baba, Y. Senoh, H. Kimura-Suda, S.B. Sato, N. Terada, S. Ohno, E. Kiyokawa, M. Umera, T. Kobayashi, Oligomerization and pore formation of a sphingomyelin-specific toxin, lysenin, J. Biol. Chem. 278 (2003) 22762–22770.
[27] R. Ishitsuka, T. Kobayashi, Cholesterol and lipid/protein ratio control the oligomerization of a sphingomyelin-specific toxin, lysenin, Biochemistry 46 (2007) 1495–1502.
[28] K. Kwiatkowska, R. Hordejuk, P. Szymczyk, M. Kulma, A.B. Abdel-Shakor, A. Płocienniczak, K. Dolowy, A. Szewczyk, A. Sobota, Lysenin-His, a sphingomyelin-recognizing toxin, requires tryptophan 20 for cation-selective channel assembly but not for membrane binding, Mol. Membr. Biol. 24 (2007) 121–134.
[29] Y. Sekizawa, T. Kubo, H. Kobayashi, T. Nakajima, S. Natori, Molecular cloning of cDNA for lysenin, a novel protein in the earthworm *Eisenia foetida* that causes contraction of rat vascular smooth muscle, Gene 191 (1997) 97–102.
[30] E. Kiyokawa, T. Baba, N. Otsuka, A. Makino, S. Ohno, T. Kobayashi, Spatial and functional heterogeneity of sphingolipid-rich membrane domains, J. Biol. Chem. 280 (2005) 24072–24084.
[31] M. Hereć, M. Gagoś, M. Kulma, K. Kwiatkowska, A. Sobota, W.I. Gruszecki, Secondary structure and orientation of the pore-forming toxin lysenin in a sphingomyelin-containing membrane, Biochim. Biophys. Acta 1778 (2008) 872–879.
[32] S. Rufini, P. Cesaroni, A. Desideri, R. Farias, F. Gubensek, J.M. Gutiérrez, P. Luly, R. Massoud, R. Morero, J.Z. Pedersen, Calcium ion independent membrane leakage induced by phospholipase-like myotoxins, Biochemistry 31 (1992) 12424–12430.
[33] E. Szymańska, M. Korzeniowski, P. Raynal, A. Sobota, K. Kwiatkowska, Contribution of PIP-5 kinase Iα to raft-based FcγRIIA signaling, Exp. Cell. Res. 315 (2009) 981–995.
[34] E.M.M. Manders, F.J. Verbeek, J.A. Aten, Measurement of co-localization of objects in dual-colour confocal images, J. Microscopy 169 (1993) 375–382.
[35] M. Korzeniowski, K. Kwiatkowska, A. Sobota, Insights into the association of FcγRII and TCR with detergent-resistant membrane domains: isolation of the domains in detergent-free density gradients facilitates membrane fragment reconstitution, Biochemistry 42 (2003) 5358–5367.
[36] P.R. Maulik, G.G. Shipley, N-palmitoyl sphingomyelin bilayeres: structure and interactions with cholesterol and dipalmitoylphosphatidylcholine, Biochemistry 35 (1996) 8025–8034.
[37] H.A. Rinia, M.M.E. Snel, J.P.J.M. van der Eerde, B. de Kruijff, Visualizing detergent resistance domains in model membranes with atomic force microscopy, FEBS Lett. 501 (2001) 92–96.
[38] C. Yuan, J. Furlong, P. Burgos, L.J. Johnston, The size of lipid rafts: an atomic force microscopy study of ganglioside GM1 domains in sphingomyelin/DOPC/cholesterol membranes, Biophys J. 82 (2002) 2526–2535.
[39] J.C. Lawrence, D.E. Saslowsky, J.M. Edwardson, R.M. Henderson, Real-time analysis of the effects of cholesterol on lipid raft behavior using atomic force microscopy, Biophys. J. 84 (2003) 1827–1832.
[40] H. Ohvo-Rekila, B. Ramstedt, P. Leppimaki, J.P. Slotte, Cholesterol interactions with phospholipids in membranes, Prog. Lipid Res. 41 (2002) 66–97.
[41] R. Fabrini, A. De Luca, L. Stella, G. Mei, B. Orioni, S. Ciccone, G. Federici, M. Lo Bello, G. Ricci, Monomer–dimer equilibrium in glutathione transferases: a critical re-examination, Biochemistry 48 (2009) 10473–10482.
[42] K. Baer, I. Lisinski, M. Gompert, D. Stuhlmann, K. Schmolz, H.W. Klein, H. Al-Hasani, Activation of a GST-tagged AKT2/PKBβ, Biochim. Biophys. Acta 1725 (2005) 340–347.
[43] K. Terpe, Overview of bacterial expression systems for heterologous protein production: from molecular and biochemical fundamentals to commercial systems, Appl. Microbiol. Biotechnol. 72 (2006) 211–222.
[44] R. Philipova, M. Whitaker, Active ERK1 is dimerized in vivo: bisphosphodimers generate peak kinase activity and monophosphodimers maintain basal ERK1 activity, J. Cell Sci. 118 (2005) 5767–5776.
[45] A. Strzelecka-Kiliszek, M. Korzeniowski, K. Kwiatkowska, K. Mrozińska, A. Sobota, Activated FcγRII and signalling molecules revealed in rafts by ultra-structural observations of plasma-membrane sheets, Mol. Membr. Biol. 21:101-108.
[46] S.H. Untrach, G.G. Shipley, Molecular interactions between lecithin and sphingomyelin. Temperature- and composition-dependent phase separation, J. Biol. Chem. 252 (1977) 4449–4457.
[47] M.P. Veiga, J.L. Arrondo, F.M. Goni, A. Alonso, D. Marsh, Interaction of cholesterol with sphingomyelin in mixed membranes containing phosphatidylcholine, studied by spin-label ESR and IR spectroscopies. A possible stabilization of gel-phase sphingolipid domains by cholesterol, Biochemistry 40 (2001) 2614–2622.
[48] B. Bakrac, I. Gutierrez-Aguirre, Z. Podlesek, A.F. Sonnen, R.J. Gilbert, P. Macek, J.H. Lakey, G. Anderluh, Molecular determinants of sphingomyelin specificity of a eukaryotic pore-forming toxin, J. Biol. Chem. 283 (2008) 18665–18677.
[49] A. Barlic, I. Gutierrez-Aguirre, J.M. Caaveiro, A. Cruz, M.B. Ruiz-Arguello, J. Perez-Gil, J.M. Gonzalez-Manas, Lipid phase coexistence favors membrane insertion of equinatoxin-II, a pore-forming toxin from *Actinia equine*, J. Biol. Chem. 279 (2004) 34209-3416.
[50] K.S. Koumanov, A.B. Momchilova, P.J. Quinn, C. Wolf, Ceramides increase the activity of the secretory phospholipase A_2 and alter its fatty acid specificity, Biochem. J. 363 (2002) 45–51.
[51] J.M. Holopainen, M. Subramanian, P.K. Kinnunen, Sphingomyelinase induces lipid microdomain formation in a fluid phosphatidylcholine/sphingomyelin membrane, Biochemistry 37 (1998) 17562–17570.